An Inhomogeneous Field Surface MRI System

Christina L. Bray, Joseph P. Hornak; Rochester Institute of Technology, Rochester, NY, USA

Abstract

Magnetic resonance imaging (MRI) is typically performed by placing the imaged object within spatially homogeneous magnetic and radio frequency (RF) fields. This convention restricts MRI to system geometries which surround the imaged object with a magnet and RF coil. Many applications could benefit from a surface MRI device where magnet and RF coil are adjacent to the imaged object. We have developed a proof-of-concept surface MRI system which uses an inhomogeneous magnetic field, RF surface coil, and unique reconstruction method to produce tomographic images. Details of our unique system and reconstruction technique, along with phantom images, will be presented.

Introduction

Magnetic resonance imaging (MRI) is a well established diagnostic medical imaging technique. In the short 25 years since it was first introduced, it has gained astonishing popularity as the imaging modality of choice for investigating numerous pathologies due to its excellent soft tissue specificity and contrast [1]. The rapid acceptance of MRI comes despite the large approximately $2M capital investment in the hardware and the high per scan session price of $1k. The high costs associated with MRI may in part be attributed to the fact that one type of instrument dominates the marketplace. This instrument is the whole body, high field unit that is capable of performing a wide variety of imaging sequences on nearly all pieces of anatomy. This makes it difficult for a clinic specializing in imaging a specific anatomy to afford entry into the field. MRI might see even greater utility if smaller specialized units were commercially available. The evolution from one size fits all to specialized units is a natural evolution of the product development as was seen in the development of current day x-ray based imaging systems.

One such application for smaller specialized MRI systems might be in the area of dermatology to aid in the study of lesions immediately beneath the skin. We are exploring the possibility of using a spatially inhomogeneous magnetic field with a special geometry radio frequency (RF) coil to produce magnetic resonance images immediately beneath the surface of the imaged object [2,3]. This paper describes the theory behind our imaging technique, a proof of concept instrument, and preliminary results.

Theory

Consider a MRI system as shown in Figure 1. In this system, a permanent magnet source (Fig. 1a) produces a static field, B_o, along the Z axis and a butterfly coil [4] adjacent to the magnet surface produces a RF field, B_1. The resulting imaging sensitive region for this configuration is defined by a plane parallel to the Z axis and bisects the center of the RF coil. For a RF coil resonant at a frequency ν_o, B_o equals ν_o divided by the gyromagnetic ratio γ, in a curved surface above the magnet. Due to the requirement that $B_1 \perp B_o$, spins are only excited in an arc above the magnet and RF coil, and in the XY plane (see Fig. 1b). The thickness (Thk) of the arc is determined by the bandwidth of the excitation RF pulses and the gradient in B_o. The NMR signal as a function

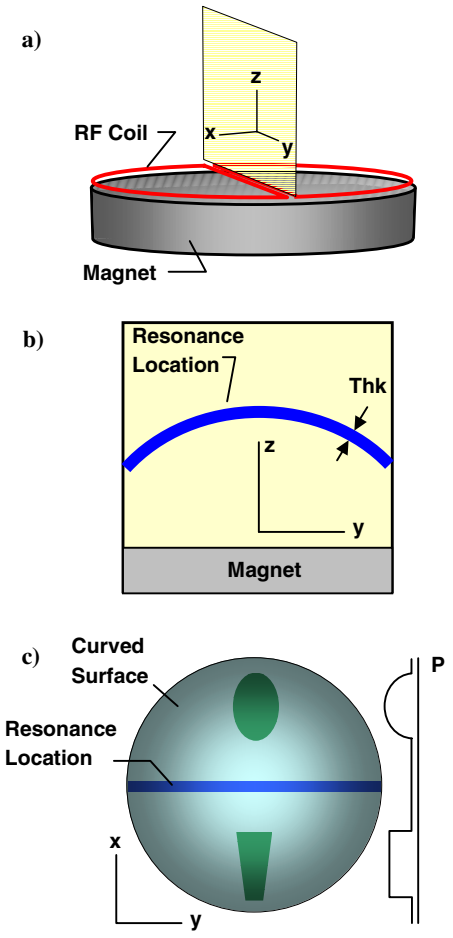

Figure 1. *Schematic representations of the a) proposed apparatus, b) resonance location in the ZY plane, and c) projection of the signal in the resonance location as the RF coil is moved along X.*

of X location of the RF coil represents the projection of the NMR signal in the curved surface onto the projection axis, P, or Y-axis in this case. (See Fig. 1c.) Varying the orientation of the RF coil in the XY-plane will produce projections at angles ϕ about Z. This 2D imaging is similar to projection imaging [5] except the imaged surface is curved. Reconstruction of the image involves warping of the result of the inverse Radon transform [6] onto the curved surface.

Experimental

To date, we have completed the characterization of various components comprising the device shown in schematic form in Figure 1a. The magnet subsystem consists of a stack of four 7.62 cm diameter by 1.27 cm thick disc rare earth (NdFeB) magnets. The RF source is a 7 cm diameter butterfly coil consisting of 7 turns of #26 Cu wire in a 2 mm thick Teflon form. A capacitance of 34 pF gives ν_o = 14.5. MHz. The thickness of the RF coil and associated ground plane sets the minimum imaging depth of 2mm.

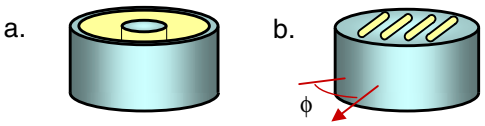

***Figure 2**. Target geometries depicting the cylinder with a symmetric zero-signal plug phantom (a), and the asymmetric four torus-slotted phantom (b).*

B_o and B_1 field performance were measured and described in further detail elsewhere [2,3]. Three-dimensional magnitude and vector maps of the B_o and B_1 fields have been generated and meet our imaging requirements for perpendicularity. A NMR spectrometer located at RIT (referred to as the host) provides the RF power source; pulse sequencing programming environment; signal detection, digitization, and processing circuitry; and file storage system.

Using our RF coil in transmit mode, a spin-echo RF-pulse sequence [7] is used to excite hydrogen proton spins along the resonant arc shown in Fig. 1b. Subsequently switching our RF coil to receive mode, the NMR signal generated from the relaxation of these exited protons is detected. The detected signal is amplified, digitized, averaged, and recorded by the host system. Translation of the RF coil in X, and rotation of the sample about Z to achieve the projections is performed mechanically.

Post processing of the acquired data is done remotely, where each integrated intensity point along the projection axis, P, is acquired and recorded. A projection ensemble is produced by mechanically rotating the test-phantom at incremental angles of above the MRI apparatus. A two-dimensional image of the test phantom is created by using a filtered inverse Radon transform reconstruction technique. This 2-D image is warped onto the resonant curved surface for the final rendering step. To produce a volume image, the resonant arc position in Z is moved and the rendering process is started over again. The resonant arc location is repositioned by either re-tuning the coil for a new resonant frequency or by moving the relative position of the RF coil with respect to the static magnet. For our current coil designs, the latter technique has been used.

Results

Several imaging phantoms have been prepared using both symmetric and asymmetric geometries using a non-signal bearing material. The voids in the material were filled with petroleum jelly, a stable, proton-rich, viscous liquid. The phantoms used for imaging consist of a simple cylinder phantom, a cylinder with a cylindrical zero-signal plug phantom, a two cylinder asymmetric phantom, and a four torus-slotted asymmetric phantom. For imaging results we will focus on the more complicated symmetric and asymmetric phantom geometries as shown in Figure 2.

The imaging results for a single projection and the 2D reconstruction for the axially symmetric plug phantom are shown in Fig. 3a and 3b, respectively. The measured projection data was prepared using 32 intensity samples collected with a 1.27 mm interval along 4 cm of P at 0°. The projection data was linearly interpolated up from 32 to 256 points prior to performing the 2D reconstruction step using 180 replicas with a 1° radial interval. Filtered backprojection reconstruction was implemented with a custom low frequency bandpass, DC reject filter. Filtering is

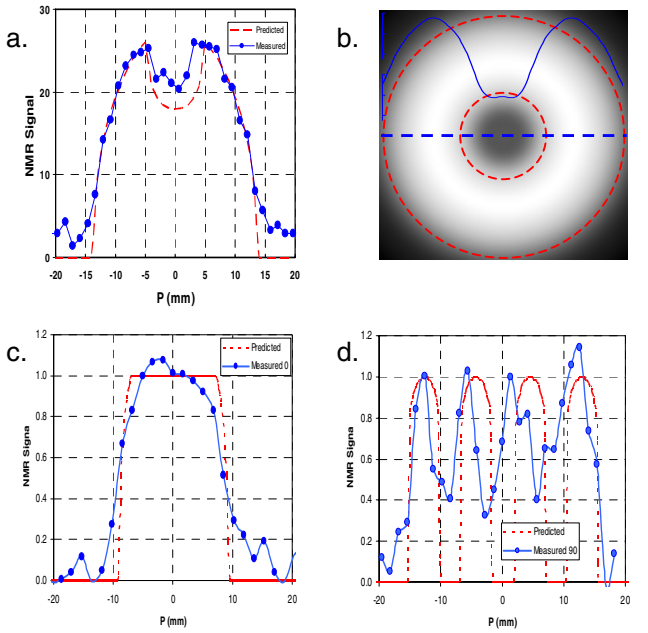

***Figure 3**. Projection results obtained from the symmetric and asymmetric phantoms shown in Fig. 2. The symmetric projection and corresponding back-projected reconstruction are shown in a. and b., respectively. Two projections for the 0° and the 90° rotations for the asymmetric phantom are depicted in c. and d. respectively.*

required to remove low frequency blurring effect caused by the backprojection process. The 2D rendering of the axially symmetric plug phantom is shown in Fig 3b, accompanied with the ideal reference (shown in red) and the preprocessed projection (shown in blue profile at 0°) used in the backprojection process.

For the axially asymmetric phantom, two projections out of a series of 6, are shown in Figs. 3c and 3d. The projection data was acquired using 27 intensity points with a 1.52 mm interval along 4 cm of P at 0° and 90°. With the current sampling used with our device, the predicted (red) and the measured (blue) projections shown in Figure 3 are in close agreement for both phantoms presented.

Conclusions

The projections and images acquired with our proof of concept apparatus present the feasibility of surface MRI using this rastered projection technique. Resolution is currently limited by the number of acquisitions in the P direction, the point spread function of the imaging sensitive portion of the transmit/receive coil, and the SNR. Furthermore, the shallow penetration depth

performance of our combined MRI system is believed to be limited to the RF power and sample digitization rate restrictions associated with the host-instrument. Further work is needed to optimize the SNR, resolution, and acquisition speed of the proof of concept apparatus as well as improving the power and sampling capabilities of the host.

Acknowledgements

The authors wish to acknowledge the contributions of Tyler Lucero for preparation and data acquisition with the asymmetric four torus-slotted phantom and James Kraus for the phantom machining.

References

[1] J. P. Hornak, The Basics of MRI, (www.cis.rit.edu/htbooks/nmr, Interactive Learning Software, Rochester, 2005).

[2] C. L. Bray, *et al*., Design and Characterization of a Sub-Surface MRI System, Proc. 15th ISMAR. (2004).

[3] C. L. Bray, *et al*., Design Iterations and Performance Enhancement for a Sub-Surface MRI System, Proc. 46th ENC. (2005).

[4] T. Munsat, W. M. Hooke, S. P. Bozeman, S. Washburnd, "Two new planar coil designs for a high pressure radio frequency plasma source", Appl. Phys. Lett. 66**,** 2185 (1995).

[5] P.G. Lauterbur, "Image formation by induced local interactions. Examples employing NMR", Nature 242**,** 190-191. (1973).

[6] S. R. Deans, The Radon Transform and Some of its Applications, (Krieger Pulishing Company, Florida, 1993), pgs. 204-217.

[7] E.L. Hahn, "Spin Echoes", Phys. Rev., 80(4), 580-584, (1950).

Author Biography

Christina Bray is an Imaging Science Ph.D. candidate at the Chester F. Carlson Center working on surface MRI. She received a BS in Chemical Engineering from the University of Rochester. Prior to joining the Magnetic Resonance Laboratory at RIT, she was a Senior Imaging Scientist with the Eastman Kodak Company in Rochester, NY. In addition to her Ph.D. research, her interests include environmental and geophysical applications of MRI, water quality, and municipal water system design.